

## Supporting Information

### **One System, Three Functions: An Electroactive Reconfigurable Organic Receptor for Adaptive Binding, Information Encoding, and Metal-Free Oxidation**

Logeshwari Seethapathy,<sup>a</sup> Rohith M.,<sup>a</sup> Chinmoy K. Hazra,<sup>b</sup> Jayanta Samanta,<sup>a</sup> Susnata Pramanik<sup>a</sup> and Rajorshi Das<sup>\*a</sup>

<sup>a</sup>Department of Chemistry, College of Engineering and Technology, SRM Institute of Science and Technology, Kattankulathur, Chennai - 603203, India.

<sup>b</sup>Department of Chemistry, Indian Institute of Technology Delhi, Hauz Khas, South Delhi – 110016, India

\*Email: [rajorshd@srmist.edu.in](mailto:rajorshd@srmist.edu.in), [rajorika@gmail.com](mailto:rajorika@gmail.com).

## Table of Contents

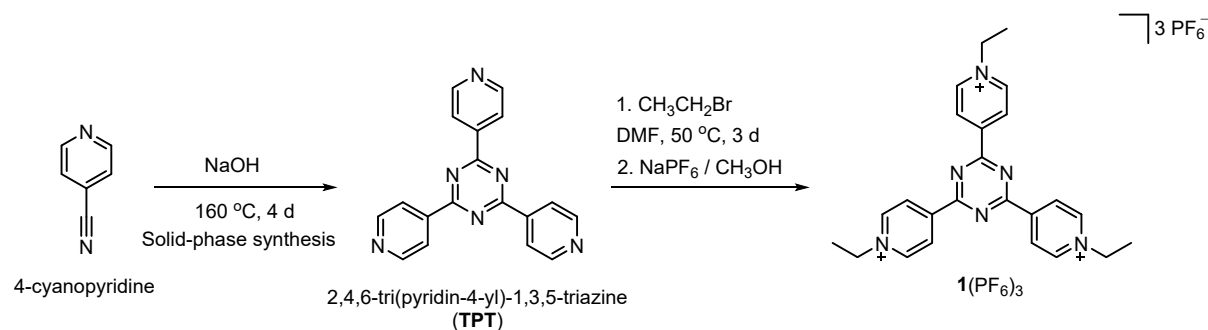
1. General Considerations	S3
2. Synthesis and Characterizations	S3
3. NMR Spectra	S7
4. ESI-MS Spectra	S12
5. X-ray Crystallographic Studies	S13
6. Electrochemical studies	S20
7. Binding constant studies	S21
8. UV-vis Spectrum	S26
9. Theoretical Calculations	S27
10. References	S31

## 1. General Considerations

All the reactions and the host-guest studies otherwise specified were performed under aerobic conditions. Starting materials were purchased from the standard commercial sources and used without further purification. Absolute solvents were prepared by distillation under a dinitrogen atmosphere prior to use for the reactions. NMR spectra were recorded at ambient temperature with Varian NMRS-500 and MR-400 spectrometers operating at 500 and 400 MHz, respectively, for  $^1\text{H}$  and  $^{13}\text{C}\{^1\text{H}\}$  NMR. High-resolution (HR) electrospray ionisation (ESI) mass spectra were obtained with a Bruker Daltonics microTOF time-of-flight mass spectrometer using an Apollo<sup>TM</sup> “ion funnel” ESI source. Mass calibration was performed immediately prior to the measurement to ensure accuracy. Solid-state UV–vis Spectra and IR spectra were obtained with a Shimadzu, UV 3600 Plus and Shimadzu, IR Tracker 100 spectrometers, respectively. Single crystals were mounted on a Bruker D8 Quest X-ray diffractometer, and the data were analysed by Apex3 software suite and further refined with Olex 2 programme.

## 2. Synthesis and characterizations

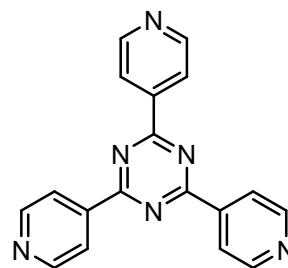
The tricationic 2,4,6-tri(4-ethylpyridyl)-1,3,5-triazinium hexafluorophosphate **1**(PF<sub>6</sub>)<sub>3</sub> was synthesized using the reaction scheme as depicted in Scheme S1.



**Scheme S1.** Synthesis of high-valent open system **1**(PF<sub>6</sub>)<sub>3</sub>.

### 2.1 Synthesis of 2,4,6-tri(4-pyridyl)-1,3,5-triazine (TPT)

To a 100 mL round bottom flask, 4-cyanopyridine (25 g, 240.384 mmol) and grounded sodium hydroxide (20 g, 500 mmol) were added. After fitting a condenser, the mixture was heated to 160 °C for 4 days. The sublimated 4-cyanopyridine was scratched down with a spatula periodically. After 4 days, the reaction mixture was cooled down to room temperature and placed on an ice bath. The alkaline mixture was



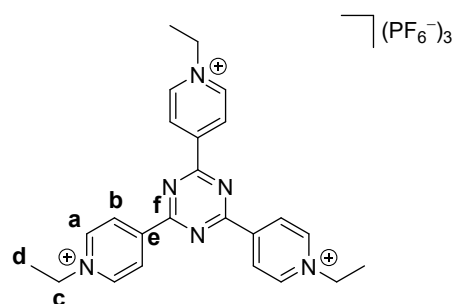
neutralized with 4N hydrochloric acid which gave a white precipitate. After filtration, the white precipitate was separated. The colourless filtrate was treated with ammonium hydroxide to precipitate the rest of the dissolved TPT from the solution, which was again filtered out. The white products were combined and evaporated to dryness under vacuum.

**Yield:** 21 g (84%, 67.234 mmol).

The NMR and ESI-MS data match with the reported literature.<sup>[1]</sup>

## 2.2 Synthesis of 2,4,6-tri(4-ethylpyridyl)-1,3,5-triazinium hexafluorophosphate 1(PF<sub>6</sub>)<sub>3</sub>

A mixture of 1 equivalent of TPT (2 g, 6.403 mmol) and 3.5 equivalent of ethyl bromide (1.7 mL, 22.4 mmol) was suspended in dry DMF (10 mL). The reaction mixture was heated under reflux at 45 °C and stirred for overnight. After 16 h, excess ethyl bromide (0.5 mL) was added, and the reaction mixture was heated under stirring at 60 °C and continued to another 2 days. The reaction mixture was cooled down to room temperature, which led to the



precipitation of a yellow coloured solid. The solid residue was washed with diethyl ether (3 x 5 mL) to remove excess ethyl bromide. After the removal of excess solvent, the residue was completely dissolved in methanol to obtain a clear saturated solution. 3.5 Equivalents of KPF<sub>6</sub> (4 g, 22.4 mmol) were added which gave an immediate formation of 2,4,6-tri(4-ethylpyridyl)-1,3,5-triazinium hexafluorophosphate 1(PF<sub>6</sub>)<sub>3</sub> as a white solid. The excess KPF<sub>6</sub> salt was removed by washing the white solid with water (3 x 5 mL). 1(PF<sub>6</sub>)<sub>3</sub> was isolated as a white solid and dried under vacuum.

**Yield:** 1.925 g (36%, 2.308 mmol).

**Yield:** 296 mg (55%, 0.355 mmol).

**<sup>1</sup>H NMR** (DMSO-*d*<sub>6</sub>):  $\delta$  (ppm) = 9.52 (br, 6H, H<sub>a</sub>), 9.48 (br, 6H, H<sub>b</sub>), 4.84 (br, 6H, H<sub>c</sub>), 1.68 (s, 9H, H<sub>d</sub>).

**<sup>13</sup>C{<sup>1</sup>H} NMR** (DMSO-*d*<sub>6</sub>):  $\delta$  (ppm) = 169.0 (C<sub>a</sub>), 148.5 (C<sub>b</sub>), 146.2 (C<sub>f</sub>), 127.1 (C<sub>e</sub>), 57.1 (C<sub>c</sub>), 16.5 (C<sub>d</sub>).

**HR-ESI MS:**  $m/z$  = 689.1559 for [1(PF<sub>6</sub>)<sub>2</sub>]<sup>+</sup> (calcd  $m/z$  = 689.1580 for C<sub>24</sub>H<sub>27</sub>F<sub>12</sub>P<sub>2</sub>N<sub>6</sub>).

**UV-vis** (solid state, nm):  $\lambda$  = 233, 300.

**IR** (ATR, cm<sup>-1</sup>):  $\nu$  = 2966 (w), 2882 (w), 1660 (w), 1545 (m), 1387 (m), 1037 (s), 855 (w), 576 (s).

### **2.3 Synthesis of the co-crystals of 2,4,6-tri(4-ethylpyridyl)-1,3,5-triazinium hexafluorophosphate $1(\text{PF}_6)_3$ with anthracene [ $1(\text{PF}_6)_3 \cdot \text{anthracene}$ ]**

Co-crystals of  $1(\text{PF}_6)_3$  with anthracene [ $1(\text{PF}_6)_3 \cdot \text{anthracene}$ ] were prepared by slow evaporation method. To a 5 mL vial,  $1(\text{PF}_6)_3$  (10 mg, 0.0120 mmol) was dissolved in 1 mL of acetonitrile. To this, anthracene (3.2 mg, 0.0180 mmol) was added into the solution. Immediate purple colour change was observed. The mixture was stirred with a sonicator until the solution became homogeneous. Subsequently, the solution was kept at rest to allow the solvent to slowly evaporate under ambient temperature. Purple coloured crystals were formed after 4 days at the bottom of the vial. The crystals were isolated and dried.

**Yield:** 8 mg (66 %, 0.0079 mmol).

### **2.4 Synthesis of the co-crystals of 2,4,6-tri(4-ethylpyridyl)-1,3,5-triazinium hexafluorophosphate $1(\text{PF}_6)_3$ with pyrene [ $1(\text{PF}_6)_3 \cdot \text{pyrene}$ ]**

Co-crystals of  $1(\text{PF}_6)_3$  with pyrene [ $1(\text{PF}_6)_3 \cdot \text{Pyrene}$ ] were prepared by slow evaporation method. To a 5 mL vial,  $1(\text{PF}_6)_3$  (10 mg, 0.0120 mmol) was dissolved in 1 mL of acetonitrile. To this, pyrene (3.64 mg, 0.0180 mmol) was added into the solution. Immediate vibrant red colour change was observed. The solution mixture was stirred with a sonicator until the solution became homogeneous. Subsequently, the solution was kept at rest to allow the solvent to slowly evaporate under room temperature. Dark brown co-crystals were formed after 3-4 days at the bottom of the vial. The crystals were isolated and dried.

**Yield:** 9 mg (72.4%, 0.0087 mmol).

### **2.5 Synthesis of the co-crystals of 2,4,6-tri(4-ethylpyridyl)-1,3,5-triazinium hexafluorophosphate $1(\text{PF}_6)_3$ with phenanthrene [ $1(\text{PF}_6)_3 \cdot \text{phenanthrene}$ ]**

Co-crystals of  $1(\text{PF}_6)_3$  and phenanthrene [ $1(\text{PF}_6)_3 \cdot \text{phenanthrene}$ ] were prepared following a similar method elaborated in 3.1 section. To a 5 mL vial,  $1(\text{PF}_6)_3$  (10 mg, 0.0120 mmol) was dissolved in 1 mL of acetonitrile. To this, phenanthrene (3.2 mg, 0.0180 mmol) was added into the solution. Immediate reddish orange colour change was observed. The mixture was stirred with a sonicator until the solution became homogeneous. Subsequently, the solution was kept at rest to allow the solvent to slowly evaporate under ambient temperature. After 4 days, orange-red crystals of  $1(\text{PF}_6)_3 \cdot \text{phenanthrene}$  were obtained at the bottom of the vial.

**Yield:** 7.3 mg (60 %, 0.0072 mmol).

### **2.6 Synthesis of the co-crystals of 2,4,6-tri(4-ethylpyridyl)-1,3,5-triazinium hexafluorophosphate $1(\text{PF}_6)_3$ with naphthalene [ $1(\text{PF}_6)_3 \cdot \text{naphthalene}$ ]**

Co-crystals of  $1(\text{PF}_6)_3$  and naphthalene [ $1(\text{PF}_6)_3 \cdot \text{naphthalene}$ ] were prepared following a similar method elaborated in 3.1 section. To a 5 mL vial,  $1(\text{PF}_6)_3$  (10 mg, 0.0120 mmol) was dissolved in 1 mL of acetonitrile. To this, naphthalene (2.3 mg, 0.0180 mmol) was added into the solution. Immediately the solution colour changed to yellow. The mixture was stirred with a sonicator until the solution became homogeneous. Subsequently, the solution was kept at rest to allow the solvent to slowly evaporate under ambient temperature. After 4-5 days, yellow crystals of  $1(\text{PF}_6)_3 \cdot \text{naphthalene}$  were obtained at the bottom of the vial. The crystals were collected and dried.

**Yield:** 7 mg (61%, 0.0073 mmol).

### **2.7 Synthesis of the co-crystals of 2,4,6-tri(4-ethylpyridyl)-1,3,5-triazinium hexafluorophosphate $1(\text{PF}_6)_3$ with perylene [ $1(\text{PF}_6)_3 \cdot \text{perylene}$ ]**

Co-crystals of  $1(\text{PF}_6)_3$  and perylene [ $1(\text{PF}_6)_3 \cdot \text{perylene}$ ] were prepared following a similar method elaborated in 3.1 section. To a 5 mL vial,  $1(\text{PF}_6)_3$  (10 mg, 0.0120 mmol) was dissolved in 2 mL of acetonitrile. To this, perylene (4.54 mg, 0.0180 mmol) was added into the solution. Immediately the solution colour changed to green. The mixture was stirred with a sonicator until the solution became homogeneous. Subsequently, the solution was kept at rest to allow the solvent to slowly evaporate under ambient temperature. After a week, bright green crystals of  $1(\text{PF}_6)_3 \cdot \text{perylene}$  were obtained. The crystals were collected and dried.

**Yield:** 9.6 mg (74 %, 0.0088 mmol).

### **2.8 Synthesis of the co-crystals of 2,4,6-tri(4-ethylpyridyl)-1,3,5-triazinium hexafluorophosphate $1(\text{PF}_6)_3$ with coronene [ $1(\text{PF}_6)_3 \cdot \text{coronene}$ ]**

Co-crystals of  $1(\text{PF}_6)_3 \cdot \text{coronene}$  were prepared following a similar method elaborated in 3.1 section. To a 5 mL vial,  $1(\text{PF}_6)_3$  (10 mg, 0.0120 mmol) was dissolved in 2 mL of acetonitrile. To this, coronene (5.4 mg, 0.0180 mmol) was added into the solution. Immediately the solution colour changed to purple-pink. The mixture was stirred with a sonicator until the solution became homogeneous. Subsequently, the solution was allowed to rest for a week to slowly evaporate the solvent under ambient temperature. After two weeks, bright green crystals of  $1(\text{PF}_6)_3 \cdot \text{coronene}$  were obtained. The crystals were collected and dried.

Yield: 5 mg (36%, 0.0044 mmol).

### 3.1 NMR Spectra

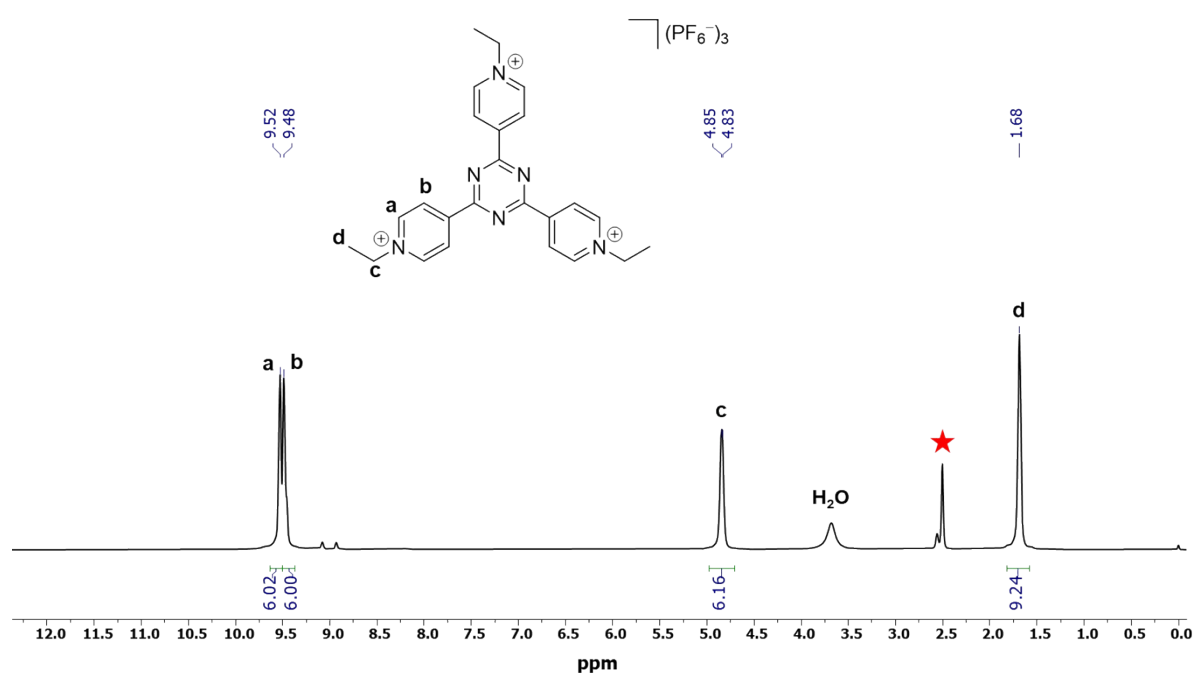


**Figure S1.** <sup>1</sup>H NMR Spectrum of [1(PF<sub>6</sub>)<sub>3</sub>] (500 MHz, DMSO-*d*<sub>6</sub>, 298 K). The solvent signal is denoted as red star.

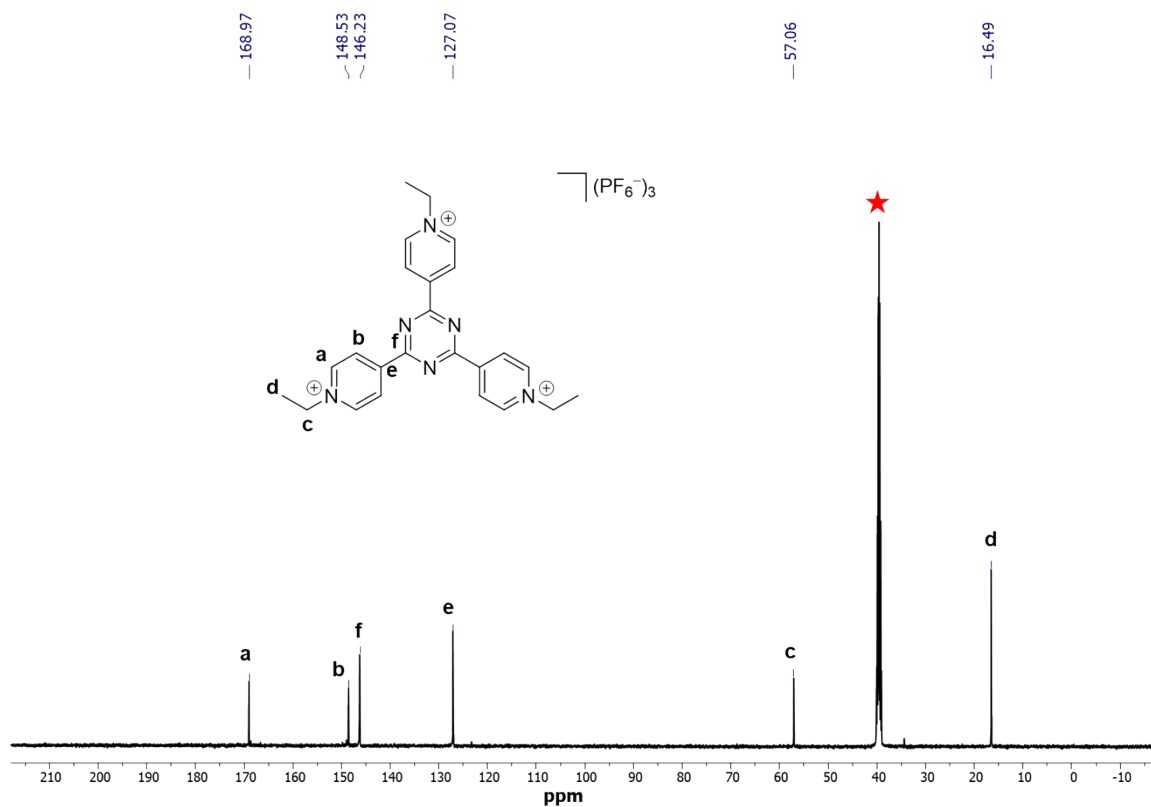


**Figure S2.**  $^{13}\text{C}$   $\{^1\text{H}\}$  NMR Spectrum of  $[\mathbf{1}(\text{PF}_6)_3]$  (125 MHz,  $\text{DMSO-}d_6$ , 298 K). The solvent signal is denoted as red star.

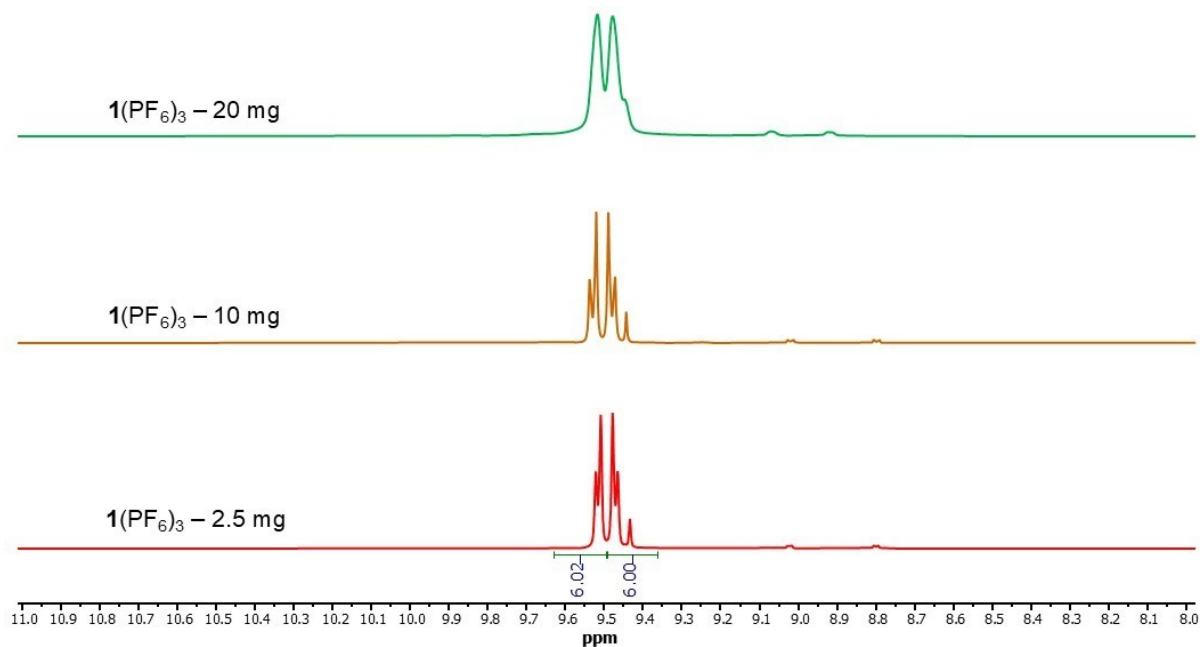


**Figure S3.** Concentration-dependent behavioural change of  $\mathbf{1}(\text{PF}_6)_3$  monitored by  $^1\text{H}$  NMR spectroscopy (400 MHz, 298K,  $\text{DMSO-}d_6$ ).

### 3.2 NMR Spectra from 'host-guest' studies

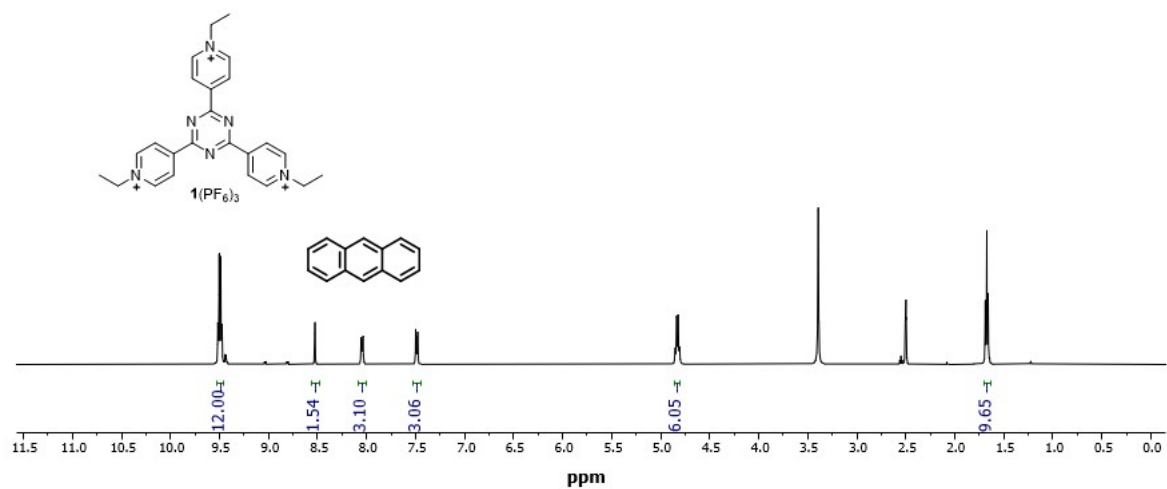


**Figure S4.**  $^1\text{H}$  NMR Spectrum obtained from the co-crystals of  $\mathbf{1}(\text{PF}_6)_3 \cdot \text{anthracene}$  (400 MHz,  $\text{DMSO-}d_6$ , 298 K).

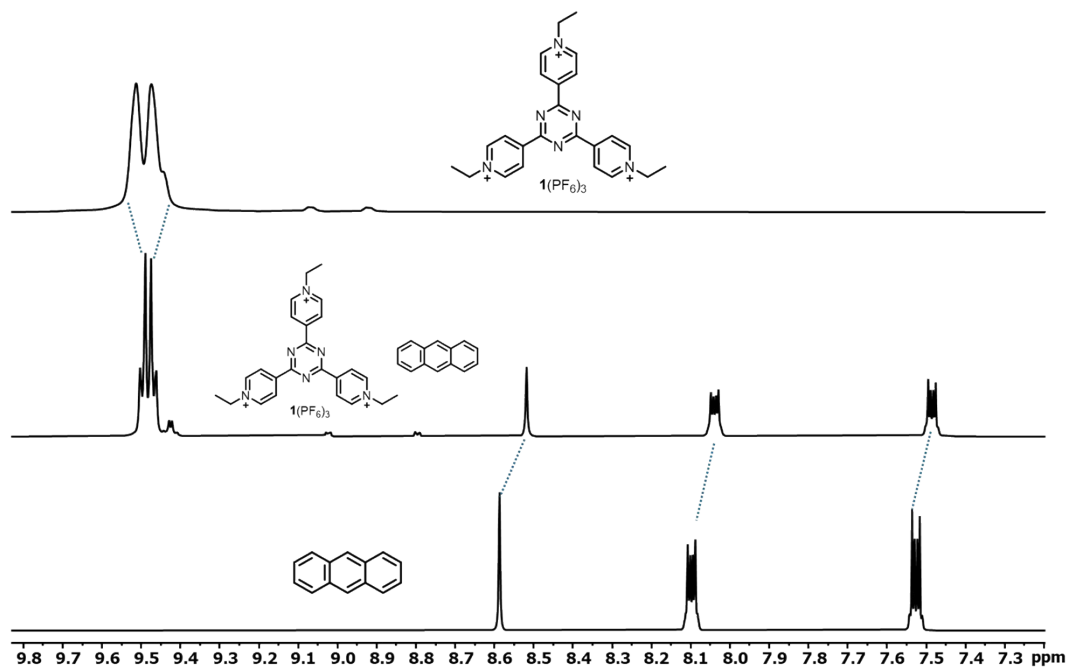


**Figure S5.** Monitoring the donor-acceptor interactions by  $^1\text{H}$  NMR spectroscopy (400 MHz, 298 K). The significant upfield shift was observed for anthracene protons compared to pyridinium protons of  $\mathbf{1}(\text{PF}_6)_3$  after complexation.

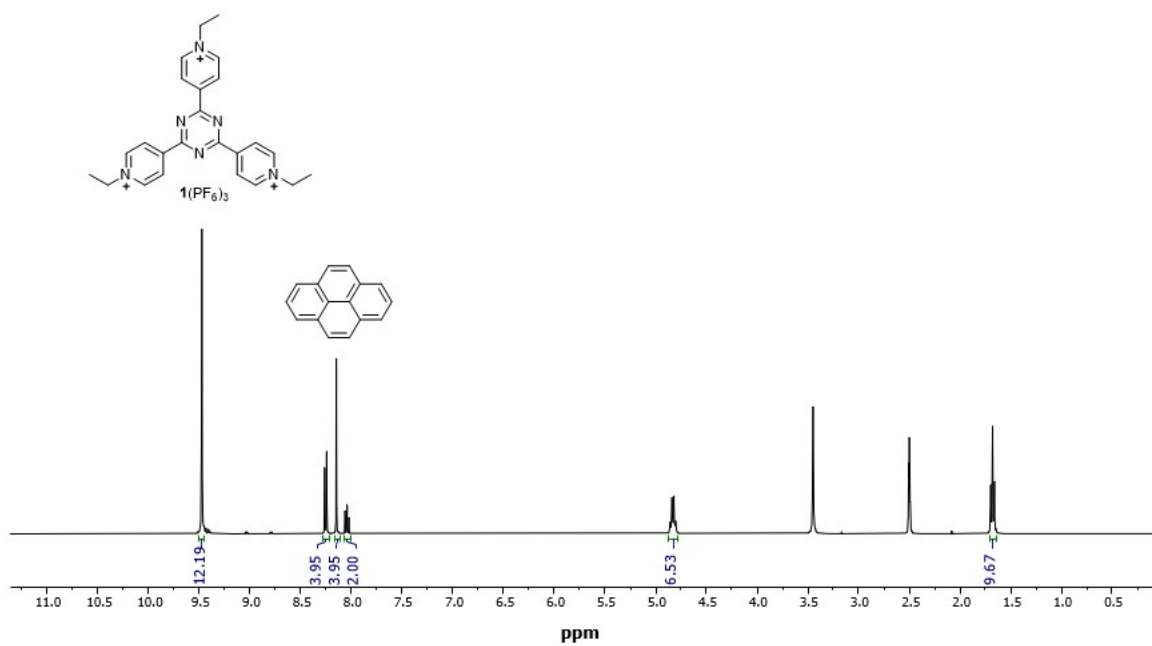


**Figure S6.**  $^1\text{H}$  NMR Spectrum obtained from the co-crystals of  $\mathbf{1}(\text{PF}_6)_3 \cdot \text{pyrene}$  (400 MHz,  $\text{DMSO-}d_6$ , 298 K).

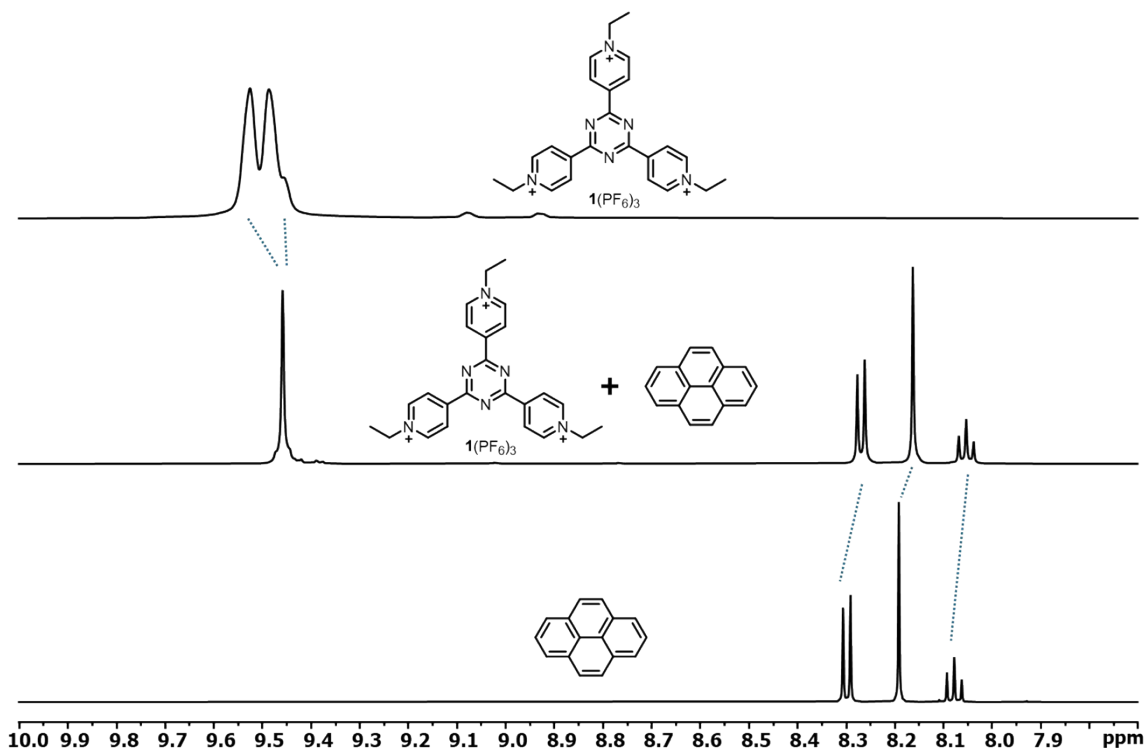


**Figure S7.** Monitoring the donor-acceptor interactions by  $^1\text{H}$  NMR spectroscopy (400 MHz, 298 K). The significant upfield shift was observed for pyrene protons compared to pyridinium protons of  $\mathbf{1}(\text{PF}_6)_3$  after complexation.

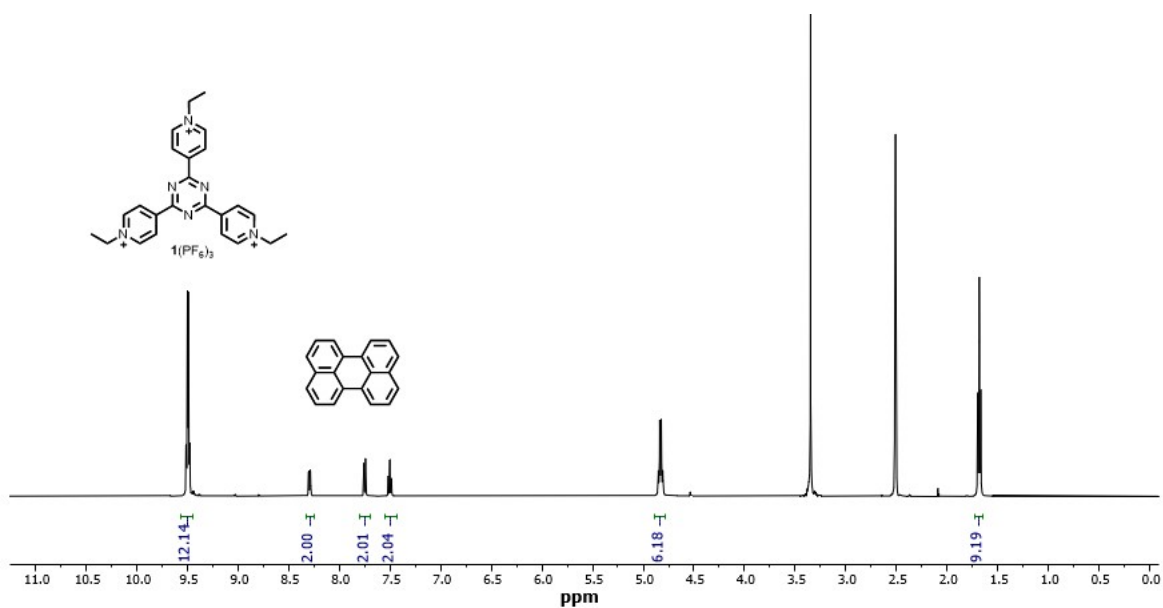


**Figure S8.**  $^1\text{H}$  NMR Spectrum obtained from the co-crystals of  $\mathbf{1}(\text{PF}_6)_3 \cdot \text{perylene}$  (400 MHz,  $\text{DMSO-}d_6$ , 298 K).

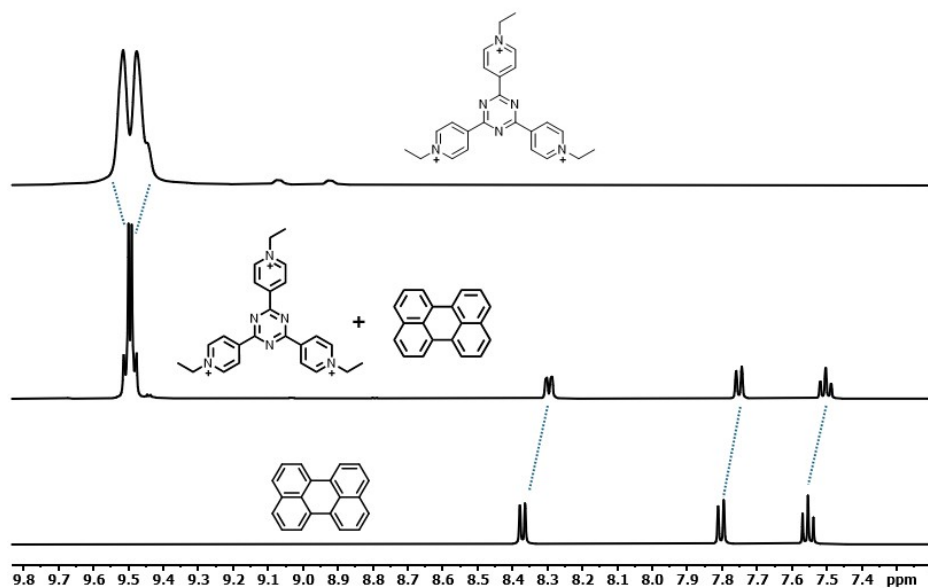


**Figure S9.** Monitoring the donor-acceptor interactions by <sup>1</sup>H NMR spectroscopy (400 MHz, 298 K). The significant upfield shift was observed for pyrene protons compared to pyridinium protons of **1**(PF<sub>6</sub>)<sub>3</sub> after complexation.

### 3.3 <sup>1</sup>H NMR Titration with **1**(PF<sub>6</sub>)<sub>3</sub> and pyrene

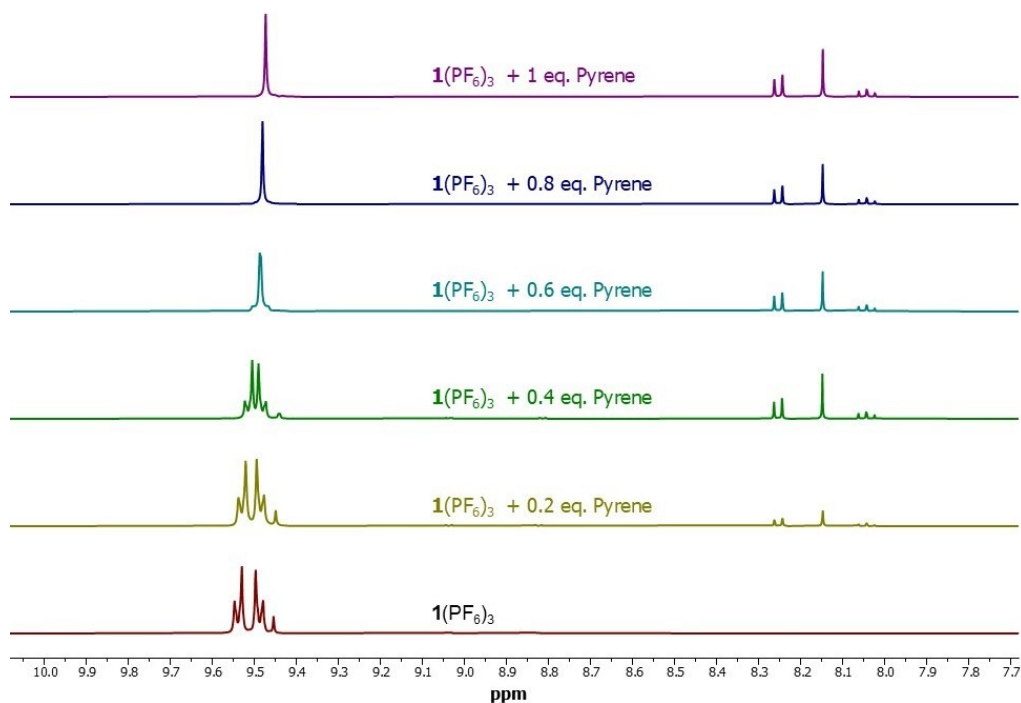


**Figure S10.** <sup>1</sup>H NMR titration of **1**(PF<sub>6</sub>)<sub>3</sub> (10 mg in 0.5 mL DMSO-*d*<sub>6</sub>, 1 equiv) with pyrene (0.2 – 1 equiv, 0.5 mg – 2.5 mg) at 298 K, 400 MHz.

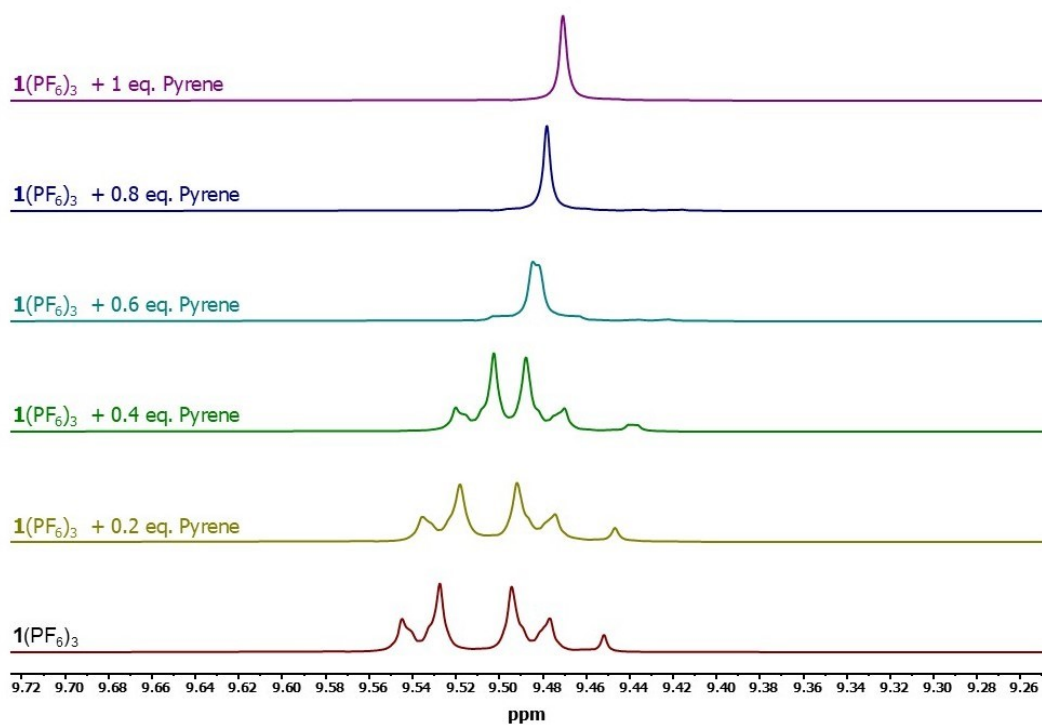


**Figure S11.** Selected portion of  $^1\text{H}$  NMR spectra (from Figure S10) obtained from titration of  $1(\text{PF}_6)_3$  (10 mg in 0.5 mL  $\text{DMSO-}d_6$ , 1 equiv) with pyrene (0.2 – 1 equiv, 0.5 mg – 2.5 mg) at 298 K, 400 MHz. The spectra show the significant change of host signals in the presence of pyrene guest.

#### 4. HR-ESI-MS Spectrum

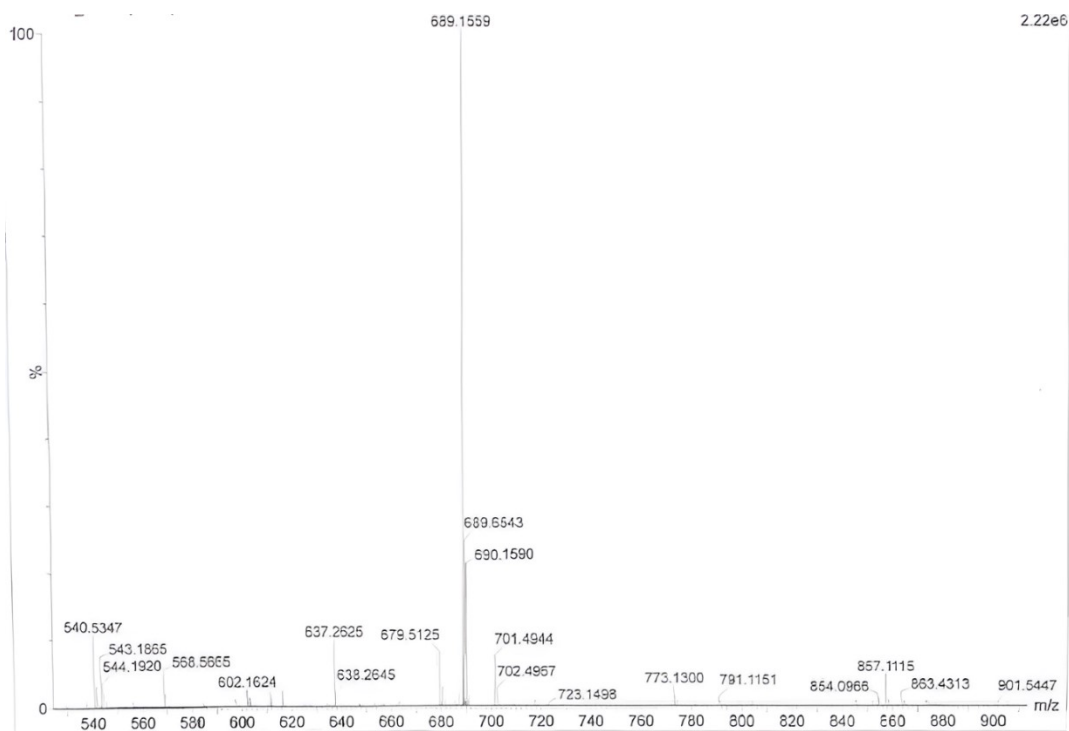


**Figure S12.** HR-ESI-MS spectrum of  $1(\text{PF}_6)_3$  in acetonitrile (+ve mode).

## 5. X-ray crystallographic studies

Single crystals, suitable for X-ray diffraction analysis, were grown by slow evaporation of a concentrated solution of the compounds. Data were collected on a Bruker D8 quest diffractometer with MoK $\alpha$  ( $\lambda = 0.71073$ ) radiation. Preliminary lattice parameters and orientation matrices were obtained from three sets of frames. Then full data were collected using the  $\omega$  and  $\phi$  scan method with a frame width of  $0.5^\circ$ . Data were processed with the SAINT+ program for reduction and cell refinement. Multi-scan absorption corrections were applied by using the SADABS program for area detector.<sup>[2]</sup> The structures were solved by SHELXT<sup>[3]</sup> and refined with SHELXL<sup>[4]</sup> using Olex2 program.<sup>[5]</sup> Most of the PF<sub>6</sub><sup>-</sup> anions are found in two-fold disorder and accordingly, similar bond distance (SADI), similar  $U_{ij}$  (SIMU), and rigid body restraints (RIGU) were applied. Phenanthrene and pyrene molecules were also found in two-fold disorder and treated with the above mentioned restraints. The CIFs are submitted to CCDC (2476293-2476297) and can be obtained free of charge via the joint Cambridge Crystallographic Data Centre (CCDC) and Fachinformationszentrum Karlsruhe through <https://summary.ccdc.cam.ac.uk/structure-summary-form>.

### Crystallization and details

**1(PF<sub>6</sub>)<sub>3</sub>**: Slow evaporation of solvent at ambient temperature from a saturated solution of **1(PF<sub>6</sub>)<sub>3</sub>** in acetonitrile or dimethylformamide yielded needle and block-shaped colourless crystals of **1(PF<sub>6</sub>)<sub>3</sub>**.

**Crystallization of all donor-acceptor complexes {1(PF<sub>6</sub>)<sub>3</sub>•anthracene, 1(PF<sub>6</sub>)<sub>3</sub>•phenanthrene and 1(PF<sub>6</sub>)<sub>3</sub>•pyrene}**: 1.5 equiv. of donors were added to an acetonitrile solution of **1(PF<sub>6</sub>)<sub>3</sub>**. The solution was sonicated to completely dissolve the donors. In case of undissolved donors, slightly excess amount of acetonitrile or dimethylformamide was added into the solution to prepare a saturated solution. Subsequently, the solutions were allowed to slowly evaporate at an ambient temperature, which resulted in the good quality single-crystals.

**[DMFC]PF<sub>6</sub>**: The addition of equivalent amount of decamethylferrocene into the acetonitrile solution of **1(PF<sub>6</sub>)<sub>3</sub>** immediately formed light green solution. The vial containing the oxidized ferrocenium hexafluorophosphate was then kept under a nitrogen atmosphere. The slow evaporation of acetonitrile from that solution yielded single crystals in 3-4 days.

**Table 1.** Crystal data and structure refinement for **1**(PF<sub>6</sub>)<sub>3</sub>

CCDC No.	2476293
Identification code	TETPT_0m
Empirical formula	C <sub>12</sub> H <sub>13.5</sub> F <sub>9</sub> N <sub>3</sub> P <sub>1.5</sub>
Formula weight	417.21
Temperature/K	273.15
Crystal system	trigonal
Space group	<i>R</i> 3m
<i>a</i> /Å	18.329(7)
<i>b</i> /Å	18.329(7)
<i>c</i> /Å	8.653(3)
$\alpha$ /°	90
$\beta$ /°	90
$\gamma$ /°	120
Volume/Å <sup>3</sup>	2518(2)
<i>Z</i>	6
$\rho_{\text{calc}}$ /cm <sup>3</sup>	1.651
$\mu$ /mm <sup>-1</sup>	0.306
<i>F</i> (000)	1260.0
Crystal size/mm <sup>3</sup>	0.1 × 0.05 × 0.02
Radiation	MoK $\alpha$ ( $\lambda$ = 0.71073)
2 $\Theta$ range for data collection/°	4.444 to 50.006
Index ranges	-21 ≤ <i>h</i> ≤ 21, -21 ≤ <i>k</i> ≤ 21, -10 ≤ <i>l</i> ≤ 10
Reflections collected	8853
Independent reflections	1090 [ <i>R</i> <sub>int</sub> = 0.0506, <i>R</i> <sub>sigma</sub> = 0.0356]
Data/restraints/parameters	1090/551/113
Goodness-of-fit on <i>F</i> <sup>2</sup>	1.085
Final <i>R</i> indexes [ <i>I</i> ≥ 2 $\sigma$ ( <i>I</i> )]	<i>R</i> <sub>1</sub> = 0.0479, <i>wR</i> <sub>2</sub> = 0.1292
Final <i>R</i> indexes [all data]	<i>R</i> <sub>1</sub> = 0.0489, <i>wR</i> <sub>2</sub> = 0.1307
Largest diff. peak/hole / e Å <sup>-3</sup>	0.34/-0.26
Flack parameter	0.12(6)

**Table 2.** Crystal data and structure refinement for **1**(PF<sub>6</sub>)<sub>3</sub>•anthracene.

CCDC No	2476294
Identification code	TETANT_a
Empirical formula	C <sub>38</sub> H <sub>37</sub> F <sub>18</sub> N <sub>6</sub> P <sub>3</sub>
Formula weight	1012.64
Temperature/K	273.15
Crystal system	monoclinic
Space group	<i>P</i> 2 <sub>1</sub> / <i>c</i>
<i>a</i> /Å	14.650(6)
<i>b</i> /Å	24.299(9)
<i>c</i> /Å	13.101(4)
$\alpha$ /°	90
$\beta$ /°	110.995(11)
$\gamma$ /°	90
Volume/Å <sup>3</sup>	4354(3)
<i>Z</i>	4
$\rho_{\text{calc}}$ /cm <sup>3</sup>	1.545
$\mu$ /mm <sup>-1</sup>	0.251
<i>F</i> (000)	2056.0
Crystal size/mm <sup>3</sup>	0.31 × 0.11 × 0.09
Radiation	MoK $\alpha$ ( $\lambda$ = 0.71073)
2 $\Theta$ range for data collection/°	3.958 to 53.69
Index ranges	-16 ≤ <i>h</i> ≤ 18, -29 ≤ <i>k</i> ≤ 30, -16 ≤ <i>l</i> ≤ 16
Reflections collected	48675
Independent reflections	9069 [ <i>R</i> <sub>int</sub> = 0.0749, <i>R</i> <sub>sigma</sub> = 0.0518]
Data/restraints/parameters	9069/327/644
Goodness-of-fit on <i>F</i> <sup>2</sup>	1.038
Final <i>R</i> indexes [ <i>I</i> ≥ 2 $\sigma$ ( <i>I</i> )]	<i>R</i> <sub>1</sub> = 0.0854, <i>wR</i> <sub>2</sub> = 0.2053
Final <i>R</i> indexes [all data]	<i>R</i> <sub>1</sub> = 0.1334, <i>wR</i> <sub>2</sub> = 0.2363
Largest diff. peak/hole / e Å <sup>-3</sup>	0.45/-0.41

**Table 3.** Crystal data and structure refinement for **1**(PF<sub>6</sub>)<sub>3</sub>•phenanthrene.

CCDC No	2476295
Identification code	TETPTPHEN
Empirical formula	C <sub>38</sub> H <sub>37</sub> F <sub>18</sub> N <sub>6</sub> P <sub>3</sub>
Formula weight	1012.64
Temperature/K	273.15
Crystal system	monoclinic
Space group	<i>P</i> 2 <sub>1</sub> / <i>c</i>
<i>a</i> /Å	6.5813(4)
<i>b</i> /Å	26.6373(16)
<i>c</i> /Å	24.8163(16)
$\alpha$ /°	90
$\beta$ /°	91.357(2)
$\gamma$ /°	90
Volume/Å <sup>3</sup>	4349.3(5)
<i>Z</i>	4
$\rho_{\text{calc}}$ /g/cm <sup>3</sup>	1.546
$\mu$ /mm <sup>-1</sup>	0.252
<i>F</i> (000)	2056.0
Crystal size/mm <sup>3</sup>	0.31 × 0.17 × 0.099
Radiation	MoK $\alpha$ ( $\lambda$ = 0.71073)
2 $\Theta$ range for data collection/°	4.488 to 50.216
Index ranges	-7 ≤ <i>h</i> ≤ 7, -31 ≤ <i>k</i> ≤ 31, -28 ≤ <i>l</i> ≤ 29
Reflections collected	65769
Independent reflections	7743 [ <i>R</i> <sub>int</sub> = 0.1026, <i>R</i> <sub>sigma</sub> = 0.0539]
Data/restraints/parameters	7743/2146/826
Goodness-of-fit on <i>F</i> <sup>2</sup>	1.079
Final <i>R</i> indexes [ <i>I</i> ≥ 2 $\sigma$ ( <i>I</i> )]	<i>R</i> <sub>1</sub> = 0.1289, <i>wR</i> <sub>2</sub> = 0.2935
Final <i>R</i> indexes [all data]	<i>R</i> <sub>1</sub> = 0.1771, <i>wR</i> <sub>2</sub> = 0.3254
Largest diff. peak/hole / e Å <sup>-3</sup>	0.71/-0.56

**Table 4.** Crystal data and structure refinement for **1(PF<sub>6</sub>)<sub>3</sub>•pyrene**.

CCDC No	2476296
Identification code	TETPTPYR
Empirical formula	C <sub>40</sub> H <sub>37</sub> F <sub>18</sub> N <sub>6</sub> P <sub>3</sub>
Formula weight	1036.66
Temperature/K	273.15
Crystal system	triclinic
Space group	<i>P</i> -1
<i>a</i> /Å	6.530(2)
<i>b</i> /Å	13.125(5)
<i>c</i> /Å	26.157(10)
$\alpha$ /°	89.813(13)
$\beta$ /°	89.925(11)
$\gamma$ /°	85.934(12)
Volume/Å <sup>3</sup>	2236.2(15)
<i>Z</i>	2
$\rho_{\text{calc}}$ /cm <sup>3</sup>	1.540
$\mu$ /mm <sup>-1</sup>	0.247
<i>F</i> (000)	1052.0
Crystal size/mm <sup>3</sup>	0.37 × 0.12 × 0.09
Radiation	MoK $\alpha$ ( $\lambda$ = 0.71073)
2 $\Theta$ range for data collection/°	4.396 to 51.696
Index ranges	-7 ≤ <i>h</i> ≤ 7, -15 ≤ <i>k</i> ≤ 15, -31 ≤ <i>l</i> ≤ 31
Reflections collected	62642
Independent reflections	8381 [ <i>R</i> <sub>int</sub> = 0.1068, <i>R</i> <sub>sigma</sub> = 0.0606]
Data/restraints/parameters	8381/2305/865
Goodness-of-fit on <i>F</i> <sup>2</sup>	1.104
Final <i>R</i> indexes [ <i>I</i> ≥ 2 $\sigma$ ( <i>I</i> )]	<i>R</i> <sub>1</sub> = 0.1382, <i>wR</i> <sub>2</sub> = 0.3491
Final <i>R</i> indexes [all data]	<i>R</i> <sub>1</sub> = 0.1898, <i>wR</i> <sub>2</sub> = 0.3834
Largest diff. peak/hole / e Å <sup>-3</sup>	0.61/-0.35

**Table 5.** Crystal data and structure refinement for [DMFC]PF<sub>6</sub>.

CCDC No	2476297
Identification code	DMFCPF6
Empirical formula	C <sub>20</sub> H <sub>30</sub> F <sub>6</sub> FeP
Formula weight	471.26
Temperature/K	273.15
Crystal system	monoclinic
Space group	C2/m
<i>a</i> /Å	14.341(2)
<i>b</i> /Å	8.9089(12)
<i>c</i> /Å	9.1627(15)
$\alpha$ /°	90
$\beta$ /°	112.327(5)
$\gamma$ /°	90
Volume/Å <sup>3</sup>	1082.9(3)
<i>Z</i>	2
$\rho$ calcg/cm <sup>3</sup>	1.445
$\mu$ /mm <sup>-1</sup>	0.823
<i>F</i> (000)	490.0
Crystal size/mm <sup>3</sup>	0.14 × 0.067 × 0.064
Radiation	MoK $\alpha$ ( $\lambda$ = 0.71073)
2 $\Theta$ range for data collection/°	4.806 to 50.878
Index ranges	-17 ≤ <i>h</i> ≤ 17, -10 ≤ <i>k</i> ≤ 10, -11 ≤ <i>l</i> ≤ 11
Reflections collected	15517
Independent reflections	1061 [ <i>R</i> <sub>int</sub> = 0.0490, <i>R</i> <sub>sigma</sub> = 0.0181]
Data/restraints/parameters	1061/0/77
Goodness-of-fit on <i>F</i> <sup>2</sup>	1.176
Final <i>R</i> indexes [ <i>I</i> ≥ 2 $\sigma$ ( <i>I</i> )]	<i>R</i> <sub>1</sub> = 0.0355, <i>wR</i> <sub>2</sub> = 0.0985
Final <i>R</i> indexes [all data]	<i>R</i> <sub>1</sub> = 0.0370, <i>wR</i> <sub>2</sub> = 0.0993
Largest diff. peak/hole / e Å <sup>-3</sup>	0.51/-0.27

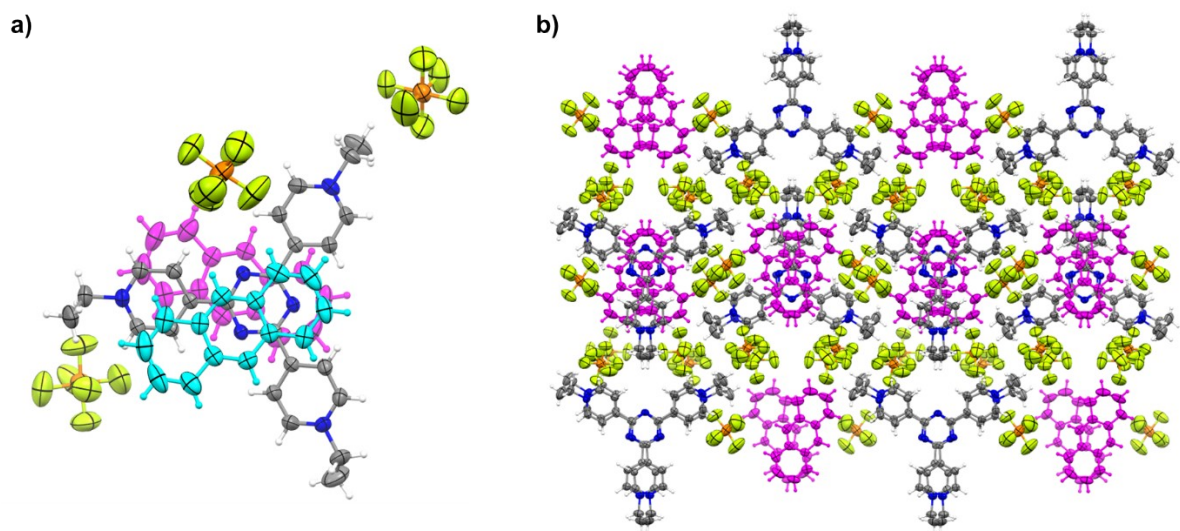


**Figure S13.** X-ray diffraction structure of 1(PF<sub>6</sub>)<sub>3</sub>•anthracene adduct. **a)** Asymmetric unit and **b)** packing structure.

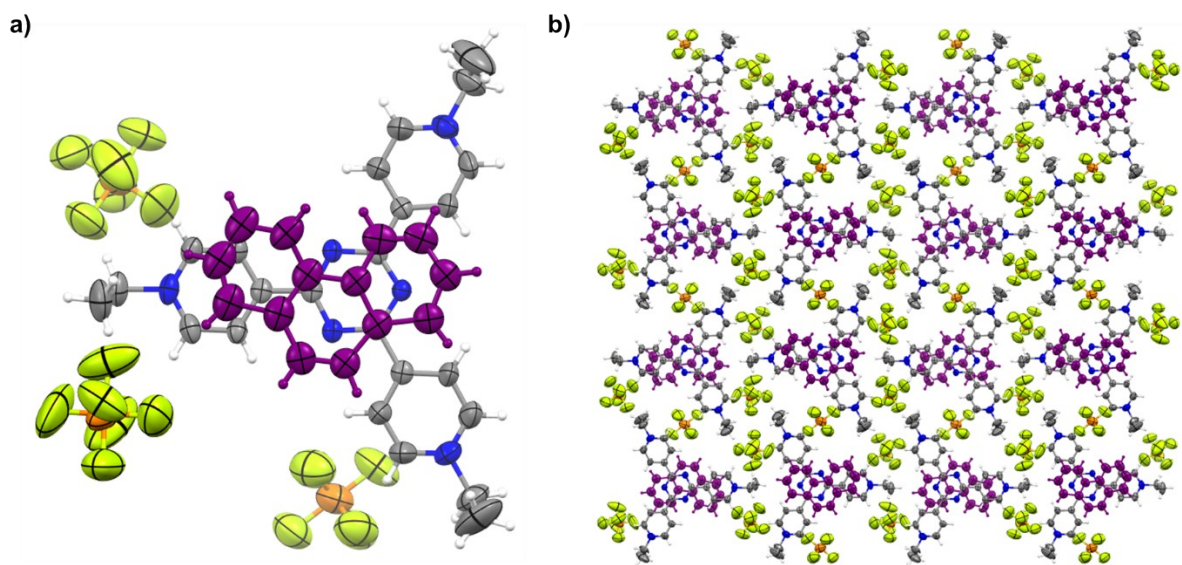


**Figure S14.** X-ray diffraction structure of 1(PF<sub>6</sub>)<sub>3</sub>•phenanthrene adduct. **a)** Asymmetric unit and **b)** packing structure.

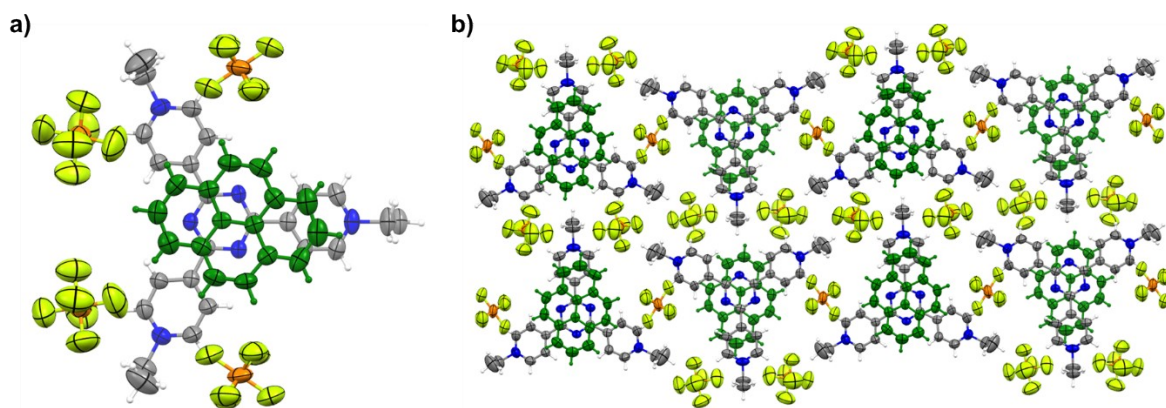


**Figure S15.** X-ray diffraction structure of  $1(\text{PF}_6)_3 \cdot \text{pyrene}$  adduct. **a)** Asymmetric unit and **b)** packing structure.

## 6. Electrochemical studies

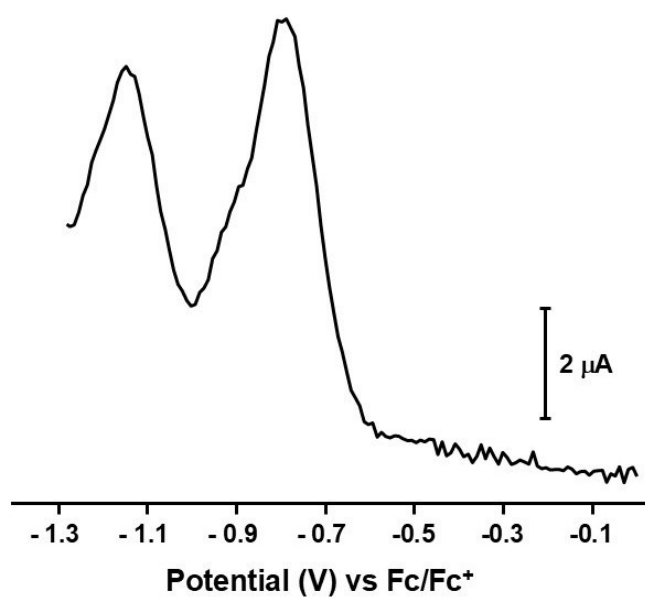


**Figure S16.** Square-wave voltammogram of  $1(\text{PF}_6)_3$  performed at a standard scan rate of 100 mV/s using  $n\text{Bu}_4\text{NPF}_6$  (0.1 M) as supporting electrolyte, referenced with  $\text{Fc}/\text{Fc}^+$  standard, and Pt wire as working electrode in dry dimethyl formamide (DMF).

## 7. Determination of binding constants

The binding constants have been calculated by monitoring the change of intensity in the photoluminescence spectroscopy. Upon gradual addition of tricationic acceptor  $1(\text{PF}_6)_3$ , the luminescence intensities of the electron-rich polyaromatic hydrocarbons reduce. For all measurements, same concentrations of the acceptor  $1(\text{PF}_6)_3$  ( $5 \times 10^{-3}$  M) and donors ( $1 \times 10^{-5}$  M) were used. Degassed acetonitrile was used in every experiment. All are conducted in the ambient temperature.  $K_{11}$  and  $K_{12}$  values are by calculated by the global fit V0.5 analysis.<sup>[6]</sup>

### 7.1 Titration of naphthalene with $1(\text{PF}_6)_3$

**Table S6. Data values from the titration study of naphthalene with  $1(\text{PF}_6)_3$**

[Naphthalene]	$1(\text{PF}_6)_3$	$1(\text{PF}_6)_3$ / [Naphthalene] (equiv.)	$I_{323 \text{ nm}}$	$I_{337 \text{ nm}}$
0.00001	0	0	327356.938	268936.84
9.9701E-06	1.4955E-05	1.5	267689.401	224553.5
9.9404E-06	2.9821E-05	3	224418.085	190682
9.9108E-06	4.4599E-05	4.5	177599.139	152138.58
9.8814E-06	5.9289E-05	6	155500.062	132282.88
9.8522E-06	7.3892E-05	7.5	127664.478	111259.19
9.8232E-06	8.8409E-05	9	95393.2727	83227.61
9.7943E-06	0.00010284	10.5	87758.3711	76219.71
9.7656E-06	0.00011719	12	76278.8772	65707.87
9.7371E-06	0.00013145	13.5	48339.3949	44684.18
9.7087E-06	0.00014563	15	37046.7195	33004.36
9.6805E-06	0.00015973	16.5	29453.384	28332.42
9.6525E-06	0.00017375	18	27527.8056	24828.47
9.6246E-06	0.00018768	19.5	18747.7837	17820.58
9.5969E-06	0.00020154	21	12168.3586	11980.67
9.5694E-06	0.00021531	22.5	10327.6736	8476.72

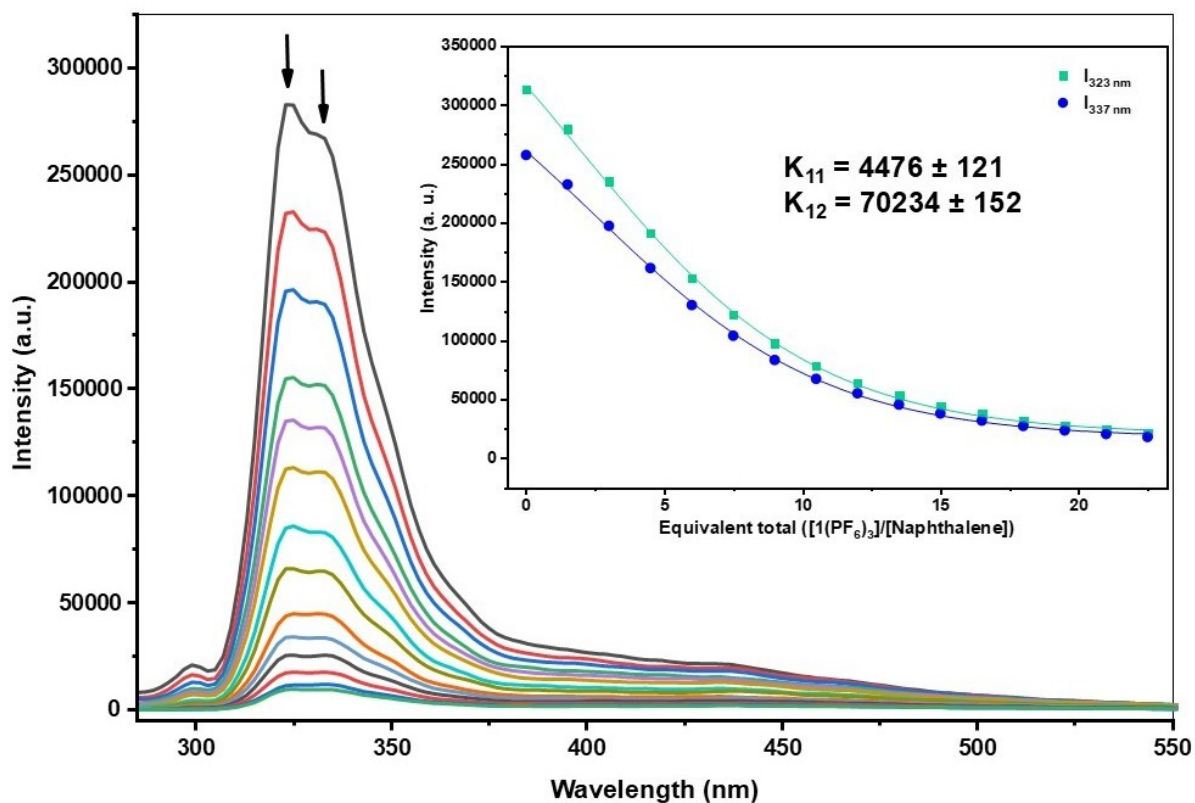


**Figure S17.** Photoluminescence titration between  $1(\text{PF}_6)_3$  and naphthalene (inset: fitting curve with scattered plot for binding constant measurement with their  $K_{11}$  and  $K_{12}$  values).  $K_{11}$  and  $K_{12}$  values are by calculated using the highest intense peak.

## 7.2 Titration of anthracene with $1(\text{PF}_6)_3$

**Table S7.** Data values from the titration study of anthracene with  $1(\text{PF}_6)_3$

[Anthracene]	$1(\text{PF}_6)_3$	$1(\text{PF}_6)_3/$ [anthracene] (equiv.)	$I_{378 \text{ nm}}$	$I_{399 \text{ nm}}$
0.00001	0	0	184658.343	195934.192
9.901E-06	4.9505E-05	5	176488.9	186404.856
9.8039E-06	9.8039E-05	10	169544.8	176461.171
9.7087E-06	0.00014563	15	163826.2	168198.972
9.6154E-06	0.00019231	20	156473.672	160685.299
9.5238E-06	0.0002381	25	149121.149	156234.853
9.434E-06	0.00028302	30	148304.202	149554.329
9.3458E-06	0.0003271	35	142585.573	145291.097
9.2593E-06	0.00037037	40	140951.679	139403.417
9.1743E-06	0.00041284	45	131965.3	134467.652
9.0909E-06	0.00045455	50	129514.4	128506.677

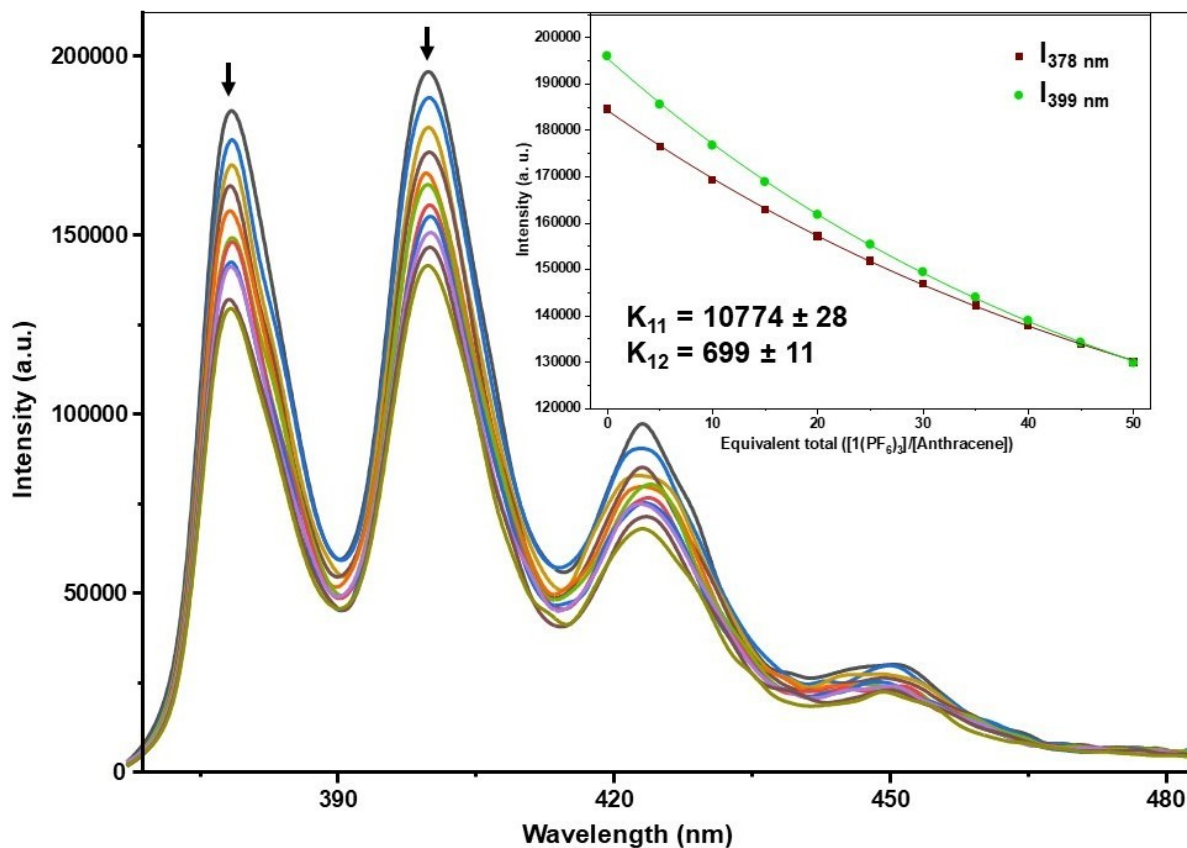


**Figure S18.** Photoluminescence titration between  $1(\text{PF}_6)_3$  and anthracene (inset: fitting curve with scattered plot for binding constant measurement with their  $K_{11}$  and  $K_{12}$  values).  $K_{11}$  and  $K_{12}$  values are by calculated using the highest intense peak.

### 7.3 Titration of pyrene with $[1(\text{PF}_6)_3]$

**Table S8.** Data values from the titration study of pyrene with  $[1(\text{PF}_6)_3]$

[Pyrene]	$[1(\text{PF}_6)_3]$	$[1(\text{PF}_6)_3]/[\text{Pyrene}]$ (equiv.)	$I_{372 \text{ nm}}$	$I_{383 \text{ nm}}$	$I_{393 \text{ nm}}$
0.00001	0	0	600543.355	358390	483849.1
9.8039E-06	9.8039E-05	10	563194.984	341431.5	463875
9.6154E-06	0.00019231	20	528850.666	327299.4	442364.4
9.434E-06	0.00028302	30	488112.362	308927.7	417781
9.2593E-06	0.00037037	40	447373.368	289142.7	391661
9.0909E-06	0.00045455	50	414044.078	272184.2	367077.5
8.9286E-06	0.00053571	60	390549.476	259465.3	354785.8
8.7719E-06	0.00061404	70	358044.196	241093.6	333275.2
8.6207E-06	0.00068966	80	325168.167	224135.1	305618.8

8.4746E-06	0.00076271	90	290643.395	205852.7	281035.3
8.3333E-06	0.00083333	100	270855.111	198930.3	267207.1
8.1967E-06	0.00090164	110	253051.916	185085.473	256451.9

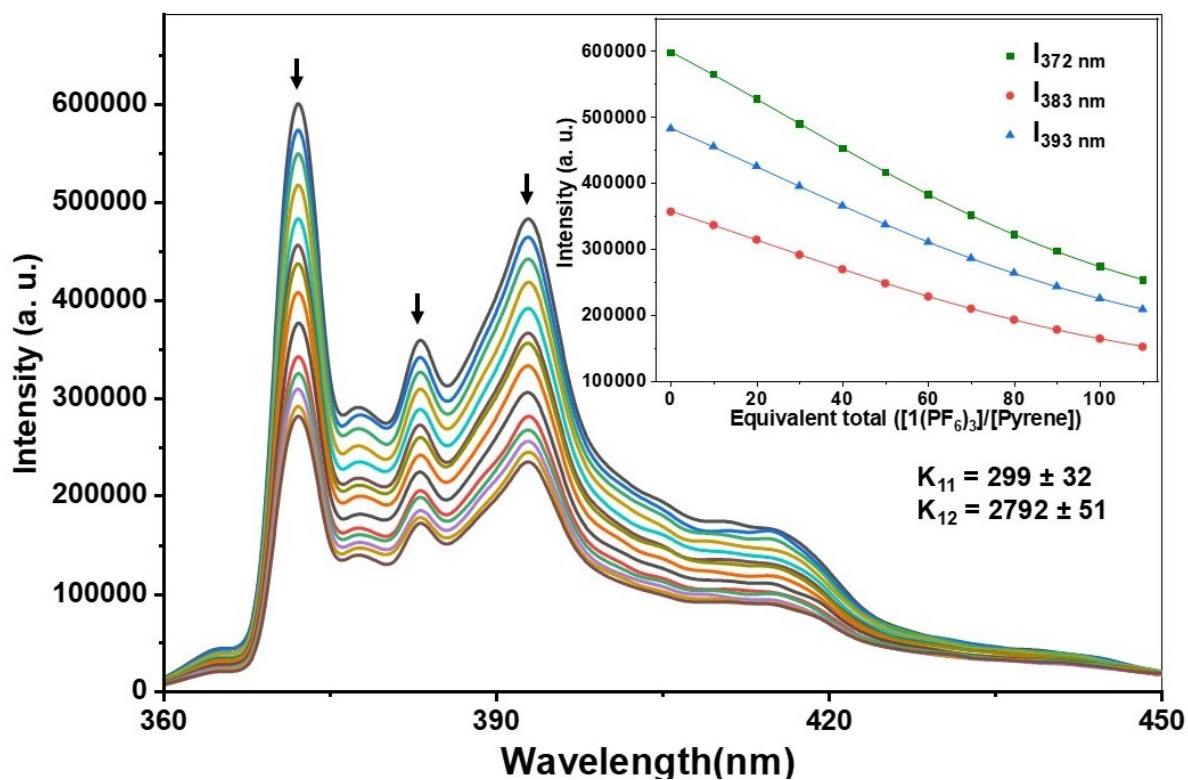


**Figure S19.** Photoluminescence titration between  $1(\text{PF}_6)_3$  and pyrene (inset: fitting curve for binding constant measurement with their  $K_{11}$  and  $K_{12}$  values).  $K_{11}$  and  $K_{12}$  values are by calculated using the highest intense peak.

#### 7.4 Titration of perylene with $[1(\text{PF}_6)_3]$

**Table S9.** Data values from the titration study of perylene with  $[1(\text{PF}_6)_3]$

[Perylene]	$[1(\text{PF}_6)_3]$	$[1(\text{PF}_6)_3] / [\text{Perylene}]$ (equiv.)	$I_{466 \text{ nm}}$
0.00001	0	0	161074.337
9.901E-06	4.9505E-05	5	156694.202
9.8039E-06	9.8039E-05	10	151376.796
9.7087E-06	0.00014563	15	147286.485
9.6154E-06	0.00019231	20	143605.204
9.5238E-06	0.0002381	25	139105.861
9.434E-06	0.00028302	30	135833.612

9.3458E-06	0.0003271	35	132970.394
9.2593E-06	0.00037037	40	127243.957
9.1743E-06	0.00041284	45	123562.677
9.0909E-06	0.00045455	50	122335.583

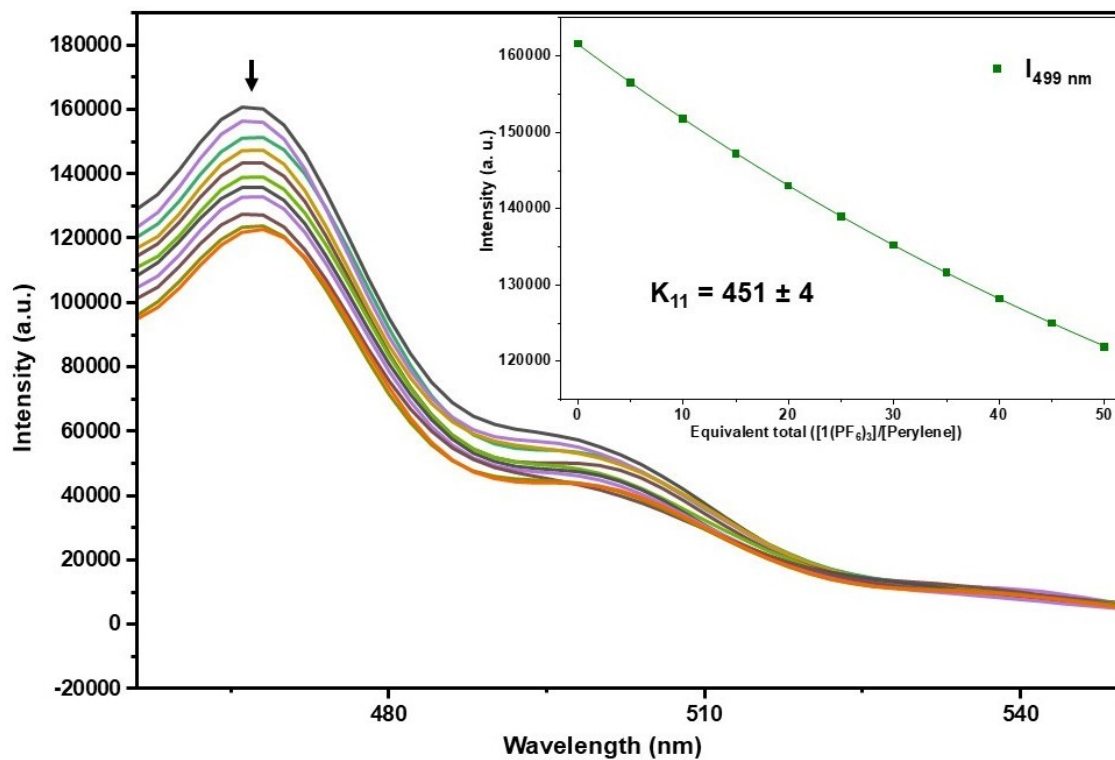


**Figure S20.** Photoluminescence titration between  $1(\text{PF}_6)_3$  and perylene (inset: fitting curve for binding constant measurement with their  $K_{11}$  value).

## 8. UV-vis Spectrum

### 8.1 Molar absorption co-efficient of $1(\text{PF}_6)_3$

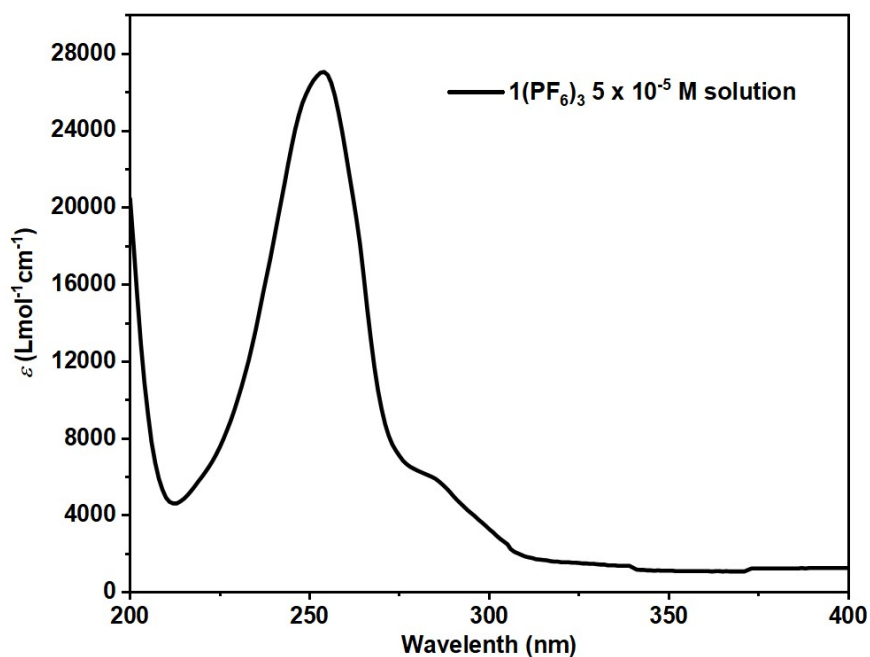


**Figure S21.** Absorption spectrum of  $1(\text{PF}_6)_3$  measured in acetonitrile ( $c = 5 \times 10^{-5} \text{ M}$ , 298 K). The molar extinction co-efficient ( $\epsilon$ ) is also calculated and included.

### 8.2 Oxidation of decamethylferrocene

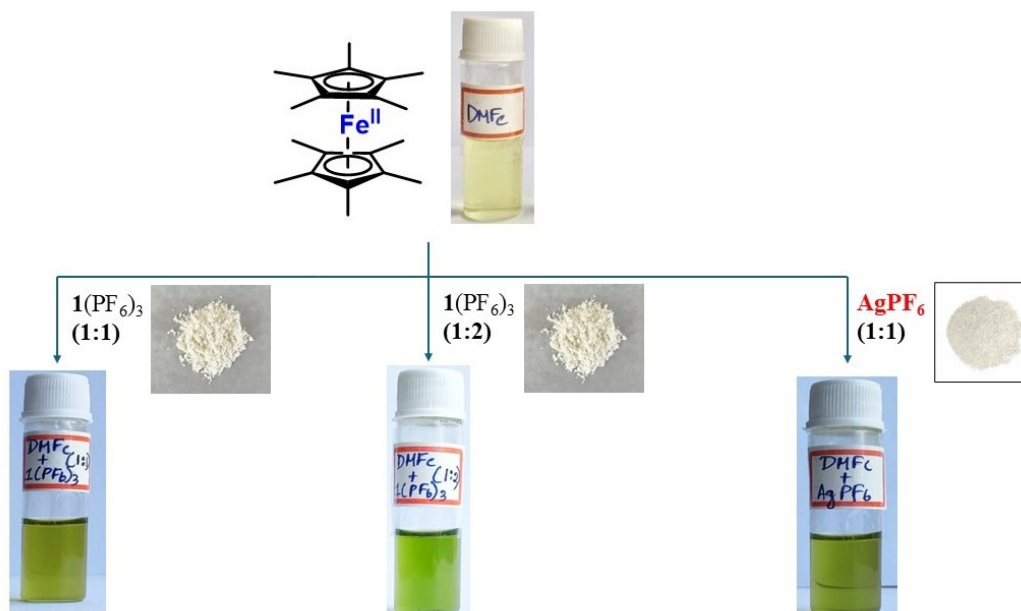


**Figure S22.** Oxidation of decamethylferrocene by  $1(\text{PF}_6)_3$  with different equivalents. The oxidation of DMFc to  $\text{DMFc}^+$  is also verified with the addition of silver hexafluorophosphate ( $\text{AgPF}_6$ ), which shows the similar color change to green.

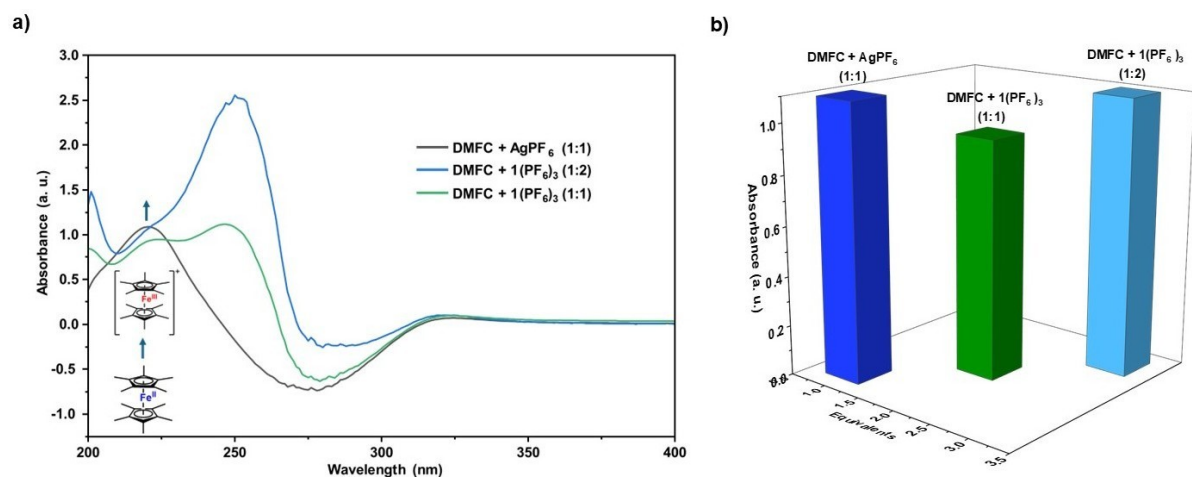


**Figure S23.** a) Monitoring the oxidation of DMFC different equivalents of  $1(\text{PF}_6)_3$  and with silver hexafluorophosphate ( $\text{AgPF}_6$ ) by UV-vis spectroscopy. b) The oxidation of DMFC to  $\text{DMFC}^+$  by  $\text{AgPF}_6$  shows the similar absorbance obtained from the 1:2 mixture of DMFC and  $1(\text{PF}_6)_3$ . Due to some technical errors, the negative absorbance was detected.

## 9. Theoretical calculations

S. N.	Functions used for calculations	Ground state energy of the bowl-shaped $[1]^{3+}$ (in HF)	Ground state energy of the planar-shaped $[1]^{3+}$ (in HF)	Energy difference (in HF)	Energy difference (in Kcal/mol)
1	b3lyp/6-311+g(d,p) (solvent=acetonitrile)	-1258.7300486	-1258.78747984	0.05743124	36.0386

### 9.1 Cartesian Coordinates of TPT

TPT (Stoichiometry:  $\text{C}_{18}\text{H}_{12}\text{N}_6$ )

SCF Done: E = -1021.91339209

-----  
Center Atomic Atomic Coordinates (Angstroms)  
Number Number Type X Y Z  
-----

1 7 0 -0.000000 1.182314 0.682528  
2 7 0 -0.000000 -1.182314 0.682528  
3 7 0 0.000000 -0.000000 -1.365319  
4 7 0 -0.000000 0.000000 5.602814  
5 7 0 0.000000 4.852405 -2.801278

6	7	0	-0.000000	-4.852405	-2.801278
7	6	0	-0.000000	0.000000	1.308405
8	6	0	0.000000	1.133181	-0.654320
9	6	0	-0.000000	-1.133181	-0.654320
10	6	0	-0.000000	0.000000	2.794147
11	6	0	0.000000	2.419916	-1.397126
12	6	0	-0.000000	-2.419916	-1.397126
13	6	0	-0.000000	1.197428	3.515455
14	6	0	0.000000	2.445976	-2.794782
15	6	0	0.000000	-3.643255	-0.720687
16	6	0	-0.000000	-1.197428	3.515455
17	6	0	0.000000	3.643255	-0.720687
18	6	0	-0.000000	-2.445976	-2.794782
19	6	0	-0.000000	1.140998	4.906079
20	6	0	0.000000	3.678557	-3.441138
21	6	0	0.000000	-4.819408	-1.464782
22	6	0	-0.000000	-1.140998	4.906079
23	6	0	0.000000	4.819408	-1.464782
24	6	0	-0.000000	-3.678557	-3.441138
25	1	0	-0.000000	2.146953	2.997949
26	1	0	0.000000	1.523073	-3.358400
27	1	0	-0.000000	-3.669794	0.360383
28	1	0	-0.000000	-2.146953	2.997949
29	1	0	0.000000	3.669794	0.360383
30	1	0	-0.000000	-1.523073	-3.358400
31	1	0	-0.000000	2.057151	5.489403
32	1	0	0.000000	3.725737	-4.526207
33	1	0	0.000000	-5.782620	-0.962960
34	1	0	-0.000000	-2.057151	5.489403
35	1	0	0.000000	5.782620	-0.962960
36	1	0	-0.000000	-3.725737	-4.526207

---

## 9.2 Cartesian Coordinates of [1]<sup>3+</sup>

[1]<sup>3+</sup> (Stoichiometry: C<sub>24</sub>H<sub>27</sub>N<sub>6</sub>(3+)) for planar conformation

SCF Done: E = -1258.78747984

-----						
Center	Atomic	Atomic	Coordinates (Angstroms)			
Number	Number	Type	X	Y	Z	
-----						
1	7	0	-5.378746	-0.789213	0.407638	
2	6	0	-2.746975	-0.403098	-0.319985	
3	6	0	-1.271478	-0.186585	-0.501182	
4	7	0	-0.512089	-1.289881	-0.483205	
5	6	0	-3.275664	-1.674688	-0.181360	
6	1	0	-2.715821	-2.444926	-0.330619	
7	6	0	-4.592828	-1.851740	0.167325	
8	1	0	-4.958694	-2.740607	0.240888	
9	6	0	-6.764895	-0.992624	0.914177	
10	1	0	-6.785372	-1.809023	1.482713	
11	6	0	-7.766786	-1.139760	-0.212452	
12	1	0	-8.668543	-1.272089	0.167606	
13	1	0	-7.761757	-0.324443	-0.769730	
14	7	0	3.372930	-4.263425	0.407645	
15	6	0	1.722575	-2.177434	-0.319976	
16	6	0	0.797297	-1.007845	-0.501175	
17	7	0	1.373032	0.201472	-0.483205	
18	6	0	3.088091	-1.999394	-0.181361	
19	1	0	3.475219	-1.129430	-0.330629	
20	6	0	3.900047	-3.051568	0.167318	
21	1	0	4.852745	-2.923966	0.240869	
22	6	0	4.242113	-5.362140	0.914180	
23	1	0	4.959436	-4.971645	1.482696	
24	6	0	4.870543	-6.156184	-0.212459	
25	1	0	5.436056	-6.871035	0.167583	
26	1	0	4.161941	-6.559530	-0.769721	
27	7	0	2.005881	5.052658	0.407651	
28	6	0	1.024381	2.580512	-0.319980	
29	6	0	0.474138	1.194400	-0.501181	
30	7	0	-0.861075	1.088366	-0.483215	
31	6	0	0.187475	3.674103	-0.181367	
32	1	0	-0.759514	3.574394	-0.330637	

33	6	0	0.692811	4.903360	0.167316
34	1	0	0.105900	5.664557	0.240870
35	6	0	2.522806	6.354798	0.914189
36	1	0	1.826041	6.780752	1.482713
37	6	0	2.896390	7.295989	-0.212449
38	1	0	3.232652	8.143187	0.167594
39	1	0	3.599876	6.884043	-0.769722
40	6	0	1.235167	-3.465370	-0.181357
41	1	0	0.299459	-3.641956	-0.330620
42	6	0	2.072396	-4.497601	0.167321
43	1	0	1.728945	-5.395335	0.240879
44	1	0	3.697287	-5.970232	1.482735
45	1	0	5.425989	-5.559466	-0.769730
46	6	0	-3.618705	0.662989	-0.181382
47	1	0	-3.303760	1.561595	-0.330656
48	6	0	-4.931209	0.454146	0.167300
49	1	0	-5.537029	1.200422	0.240846
50	1	0	-7.019055	-0.216687	1.482716
51	1	0	-7.527707	-1.919271	-0.769702
52	6	0	2.383471	2.802314	-0.181356
53	1	0	3.004234	2.080260	-0.330619
54	6	0	2.858874	4.043421	0.167328
55	1	0	3.808064	4.194929	0.240886
56	1	0	3.321899	6.186944	1.482736
57	1	0	2.101772	7.478712	-0.769709

---

## 10. References

1. H. L. Anderson, S. Anderson, J. K. M. Sanders, *J. Chem. Soc., Perkin Trans. 1* **1995**, 2231–2245.
2. (a) SADABS, v 2.05; Bruker AXS Inc.; Madison, WI, 2003; (b) G. M. Sheldrick, SAINT, version 8.37A; Bruker AXS Inc.; Madison, WI, 2013; (c) SMART, v 2.05; Bruker AXS Inc.; Madison, WI, 2003; (d) G. M. Sheldrick, SHELXT - Integrated Space-Group and Crystal Structure Determination. *Acta Crystallogr., Sect. A: Found. Adv.*, **2015**, *71*, 3–8; (e) L. J. Farrugia, WinGX and ORTEP for windows: an update. *J. Appl. Crystallogr.*, **2012**, *45*, 849–854; (f) C. F. Macrae, P. R. Edgington, P. McCabe, E. Pidcock, G. P. Shields, R. Taylor, M. Towler, J. van de Streek, *J. Appl. Crystallogr.*, **2006**, *39*, 453–457.
3. G. M. Sheldrick, *Acta Cryst.*, **2015**, *A71*, 3-8.
4. G. M. Sheldrick, *Acta Cryst.* **2015**, *C71*, 3-8.
5. O. V. Dolomanov, L. J. Bourhis, R. J. Gildea, J. A. K. Howard, H. Puschmann, *J. Appl. Cryst.*, **2009**, *42*, 339-341.
6. BindFit v0.5 | Supramolecular, <https://app.supramolecular.org/bindfit/>